Theory and analyses of the ac characteristics of defect thin-film insulators

G. S. Nadkarni and J. G. Simmons

Citation: Journal of Applied Physics **47**, 114 (1976); doi: 10.1063/1.322357
View online: http://dx.doi.org/10.1063/1.322357
View Table of Contents: http://scitation.aip.org/content/aip/journal/jap/47/1?ver=pdfcov
Published by the AIP Publishing

Theory and analyses of the ac characteristics of defect thin-film insulators*

G. S. Nadkarni† and J. G. Simmons

Electrical Engineering Department, University of Toronto, Toronto, Canada
(Received 31 January 1975, in final form 24 April 1975)

In the past, ac properties obtained from thin-film metal-insulator-metal (MIM) samples have often been analyzed *qualitatively* in terms of the Debye relaxation process. Here we point out several anomalies and discrepancies associated with these analyses. We then go on to develop the theory of ac electrical properties in MIM systems in which Schottky barriers are assumed to exist at the metal-insulator interface. The resulting capacitance and conductance vs frequency, temperature, and voltage bias are shown to exhibit all the salient features of the observed data, suggesting that such a model is more applicable than the Debye model, at least in the case of the materials reviewed.

PACS numbers: 73.40.R, 73.30., 73.60.H

I. INTRODUCTION

Recently, several papers[1-5] have been published which deal with ac conduction in the thin-film metal-insulator-metal (MIM) system. Usually it is assumed that the temperature and frequency dispersion of capacitance C, resistance R, and $\tan\delta$ as a function of temperature T and frequency ω are due to Debye-type relaxation processes. The most compelling reason for believing that this is the case is that the data appears to be expressible in terms of Cole-Cole plots.[1,2] Nevertheless, there are several anomalous features of the ac and dc conductivity which suggest that the Debye process is not necessarily the underlying mechanism involved, namely:

(i) The data fits the Cole-Cole plot over only the *high-frequency* end of the spectrum. At the low-frequency end, contrary to the Cole-Cole plot requirements, the dielectric loss actually *increases* with *decreasing* frequency.[1-5]

(ii) The ratio of the low-frequency to the high-frequency dielectric constant is found to be typically greater than 20:1, whereas, on the Debye model, a ratio of 3:1 would be more typical for most of the materials reported (e.g., SiO, Al_2O_3).

(iii) The ratio of the high-temperature to the low-temperature capacitance of the sample for a given frequency is typically 20:1,[1] whereas a *few tens of percent* would be more typical if the Debye process were applicable.

(iv) The dielectric constant appears to *increase* almost *linearly* with the thickness of the insulator, where such measurements have been made and reported.[6]

(v) There is a large change in the sample capacitance with increasing voltage bias, and the change is smaller at higher frequency or lower temperature.[1,4]

Various *ad hoc* modifications to the basic Debye equations have been invoked in an attempt to account for these anomalies. However, to date, no satisfactory self-consistent explanation has been forthcoming, as evidenced by the notable absence of any theoretically generated curves that correlate, either qualitatively or quantitatively, with the reported experimental data. Generally speaking, qualitative arguments only are used in an attempt to explain the experimental data.

All the above-stated anomalies can, in fact, be reconciled on the basis of a model in which Schottky barriers exist at the electrode-insulator interface. However, the possibility of Schottky barriers existing at the metal-insulator interface tend to be overlooked, yet such barriers are certainly possible if either traps exist throughout the insulator band gap,[7] or the insulator is autodoped during the deposition process. Indeed, it has been shown both theoretically[7-9] and experimentally[3-5,10-12] using both ac and dc techniques that Schottky barriers do exist at the metal-insulator interface in MIM systems. We will be concerned here with obtaining the theoretical ac characteristics associated with such a model. It will be seen that these characteristics show a remarkable resemblance to existing experimental data, which we believe is compelling evidence that the model is applicable to the reported data. In any case, since the existence of an interfacial Schottky barrier model has been incontrovertibly established for many MIM systems[3-5,10,11], we feel that the theory developed here must be considered in any analysis of ac experimental data of MIM systems.

II. THEORY

Throughout this paper we will be concerned primarily with developing the theoretical expressions in terms of the *observable* parameters C, R, and the dielectric constant K, rather than more esoteric parameters ϵ' and ϵ'' associated with the Debye theory. However, for the purpose of comparing the results of our model with the existing experimental data (usually expressed in Debye parameters), we will also express our results in terms of ϵ' and ϵ''.

A. Model

Figure 1(a) shows the energy-band diagram of an MIM system in which Schottky barriers exist at the metal-insulator interface.[9] The resistance of the interior of the insulator is given by

$$R_b = R_0 \exp(\phi_i/kT), \tag{1}$$

where R_0 is a resistive parameter, k is Boltzmann's constant, T is the absolute temperature, and ϕ_i is the activation energy of the neutral bulk region of the insulator.

Under steady-state conditions and low-voltage biases the reverse-biased cathodic Schottky barrier limits the current flowing in the system. Thus, the current flowing in the system is the thermionic Richardson-Schottky current associated with the cathodic barrier:

$$J = A^* T^2 \exp[(\beta F_c^{1/2} - \phi_0)/kT], \tag{2}$$

where ϕ_0 is interfacial barrier height, A^* is Richardson's constant, β is Schottky coefficient given by

$$\beta = (q^3/4\pi\epsilon_0 K)^{1/2}. \tag{3}$$

The field F_c at the cathodic interface is, for discrete level of traps or donors, given by

$$F_c = (2N_0/\epsilon_0 K)^{1/2}[\phi_0 - \phi_i + q(V - \Delta V)]^{1/2}, \tag{4}$$

where ϵ_0 is the permittivity of free space, q is the electronic charge, N_0 is the trap or donor density, V is the applied voltage, and ΔV is the portion of the applied voltage dropped across the interior of the insulator [Fig. 1(a)] and the forward-biased (anodic) barrier. Thus, the resistance of the cathodic barrier is given by

$$R_s = \frac{V - \Delta V}{J} = \frac{V - \Delta V}{A^* T^2} \exp\left(\frac{\phi_0 - \beta F_c^{1/2}}{kT}\right). \tag{5}$$

Since $\phi_0 > \phi_i$ when Schottky barriers exist at the interface, then $R_s \gg R_b$ while the conduction process is *electrode limited*. The electrode-limited conduction process does not prevail indefinitely with increasing voltage bias. This is because the resistance of the interior, Eq. (1), decreases much slower with increasing voltage bias than does that of the contact, Eq. (5). Thus, at some voltage V_T, the transition voltage, the contact resistance falls to a value equal to that of the bulk and there is an electrode-limited—to—bulk-limited transition in the conduction process.[8] When this occurs the applied voltage is shared equally between the contact and the interior. For a further increase in the voltage the majority of the voltage in excess of V_T drops across the bulk, and the remaining fraction across the barrier, the latter being just sufficient to ensure the current continuity throughout the system. Hence, for voltages in excess of V_T, the conduction process is bulk limited, that is, $R_b > R_s$.

For initial dc voltage biases $V < V_T$ applied to the system, the width λ_{sc} of the cathodic (reverse-biased) Schottky barrier grows in size according to

$$\lambda_{sc} = (2K\epsilon_0/q^2 N_0)[\phi_0 + q(V - \Delta V)]^{1/2}, \quad V < V_T. \tag{6}$$

When $V > V_T$, the width of the Schottky barrier changes very slowly with voltage, because only a small fraction of the applied voltage in excess of V_T appears across the cathodic barrier. Thus, since the capacitance of the cathodic Schottky barrier, C_{sc}, is given by

$$C_{sc} = AK\epsilon_0/\lambda_{sc},$$

where A is the sample area, then C_{sc} is voltage dependent.

The capacitance of the anodic Schottky barrier (C_{sa}) is also voltage dependent. However, since this barrier is forward biased, only a very small fraction of the applied voltage is dropped across it, the majority appearing across the reverse-biased cathodic barrier. Thus, for $V < V_T$ essentially all the applied voltage appears across the cathodic depletion region; hence, C_{sc} is much more strongly voltage dependent than C_{sa}, which varies only slightly from its zero-biased value.

B. Analysis of the equivalent circuit

The energy-band diagram shown in Fig. 1(a) can be represented by the equivalent circuit shown in Fig. 1(b). In Fig. 1(b), R_{sc}, C_{sc} and R_{sa}, C_{sa} are the resistances and capacitances of the cathodic and anodic Schottky barriers, respectively, which, of course, are voltage dependent. R_{bi} and C_{bi} represent the resistance and the capacitance of the *interior* of the insulator [see Fig. 1(a)]. For film thicknesses greater than 1000 Å and trap or impurity densities greater than 10^{17} cm^{-3}, which is generally the case, any changes in the width of the Schottky barriers are small compared to the width of the interior, so R_{bi} and C_{bi} may be assumed to be independent of the applied voltage. Thus, for the sake of analysis, the equivalent circuit in Fig. 1(b) is further simplified by lumping the essentially voltage-independent capacitances and resistances of the interior and the forward-biased anode barrier together, in the form of a single resistance R_b in parallel with a capacitor C_b, as shown in Fig. 1(c). It is noted that if the two capacitances in Fig. 1(c) were voltage independent and the resistances temperature independent, the circuit resembles the *Maxwell-Wagner* model, which comprises a uniform high-resistance layer in series with a uniform low-resistivity layer. Our model differs from the basic Maxwell-Wagner model in that it introduces the Schottky-barrier-layer and interior-layer concepts, together with their specific voltage and temperature-dependent parameters. These concepts give rise to some unique and distinguishing ac characteristics, as we will show below.

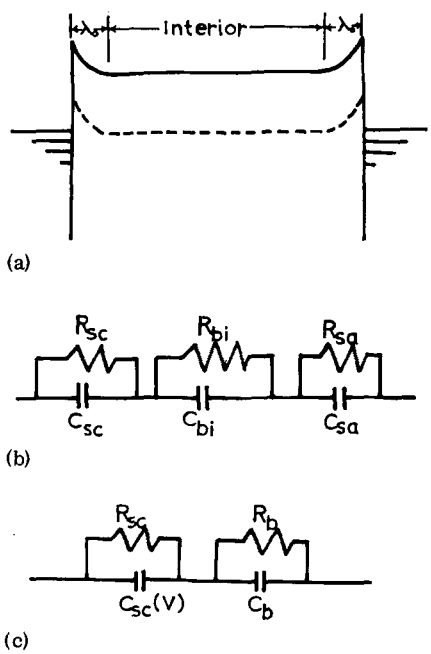

FIG. 1. (a) Energy diagram of the MIM system having Schottky barriers at the metal-insulator interface. (b) Equivalent circuit for (a). (c) Simplified equivalent circuit of (b).

The parallel equivalent capacitance of the circuit in Fig. 1(c) is given by

$$C = C_g + \frac{C_0 - C_g}{1 + (\omega T_c)^2}, \tag{8}$$

where

$$C_g = \frac{C_{sc} C_b}{C_{sc} + C_b}, \tag{9}$$

$$C_0 = \frac{C_{sc} R_{sc}^2 + C_b R_b^2}{(R_{sc} + R_b)^2}, \tag{10}$$

and

$$T_c = \frac{R_{sc} R_b}{R_{sc} + R_b} (C_{sc} + C_b). \tag{11}$$

It will be apparent from Eq. (9) that C_g is the geometric capacitance of the system. Also, from Eqs. (8) and (9) at low frequencies ($\omega T_c \ll 1$) and low voltages when $R_s \gg R_b$, C_0 is just equal to the capacitance of the Schottky barriers.

The loss tangent or tanδ of the system is given by

$$\tan\delta = (R\omega C)^{-1}. \tag{12}$$

In Eq. (12), R is the parallel-equivalent resistance of the circuit and is given by

$$R = R_1 + \frac{R_{dc} - R_1}{1 + (\omega T_R)^2}, \tag{13}$$

where

$$R_1 = \frac{R_{sc} R_b (C_{cs} + C_b)^2}{C_{sc}^2 R_{sc} + C_b^2 R_b}, \tag{14}$$

$$R_{dc} = R_{sc} + R_b, \tag{15}$$

and

$$T_R = \left(\frac{R_{sc} R_b}{R_{sc} + R_b} (C_{sc}^2 R_{sc} + C_b^2 R_b) \right)^{1/2}. \tag{16}$$

From Eqs. (13) and (15) it will be apparent that R_{dc} is the dc resistance of the system.

Equations (8), (12), and (13) may be expressed in terms of Debye parameter ϵ' and ϵ''. Thus the effective dielectric constant ϵ' is given by

$$\epsilon' = C/C_V, \tag{17}$$

where

$$C_V = A\epsilon_0/d \tag{18}$$

is the capacitance of the *system* when the dielectric is replaced by a vacuum, A is the area of the sample, and d is the thickness of the dielectric. The dielectric loss ϵ'' is given by

$$\epsilon'' = (R\omega C_V). \tag{19}$$

From Eqs. (16)—(19), we have

$$\tan\delta = \epsilon''/\epsilon'. \tag{20}$$

III. COMPARISON OF THEORY AND EXPERIMENTAL DATA

In this section we will be concerned with generating the theoretical ac characteristics and comparing them with existing experimental data. We will adopt two approaches to the problem: (i) We will present representative data obtained by the present authors that have been specifically interpreted in terms of the Schottky barrier model. (ii) We present further features of the theory and compare them with experimental data, obtained by other investigators, that has been analyzed only qualitatively (no theoretical curves were presented) in terms of Debye model. We will show that the data does, in fact, bear a strong resemblance to our theoretical curves, strongly suggesting that our model may well be applicable to the data.

A. AC properties of Au-MoO_3-Au structure

Figure 2 is a plot of capacitance-vs-inverse thickness obtained at 77 and 390 °K. At low temperatures the capacitance is inversely proportional to the thickness of the insulator, as is normally expected, and the dielectric constant obtained from the data is 15.8. This data is, thus, assumed to reflect the geometric capacitance of the samples. On the other hand, the capacitance at 390 °K is essentially thickness independent and much higher in value than that of the low-temperature capacitance of even the thinnest sample. This data may be interpreted in terms of our model as follows. At low temperatures the resistances of the Schottky barrier

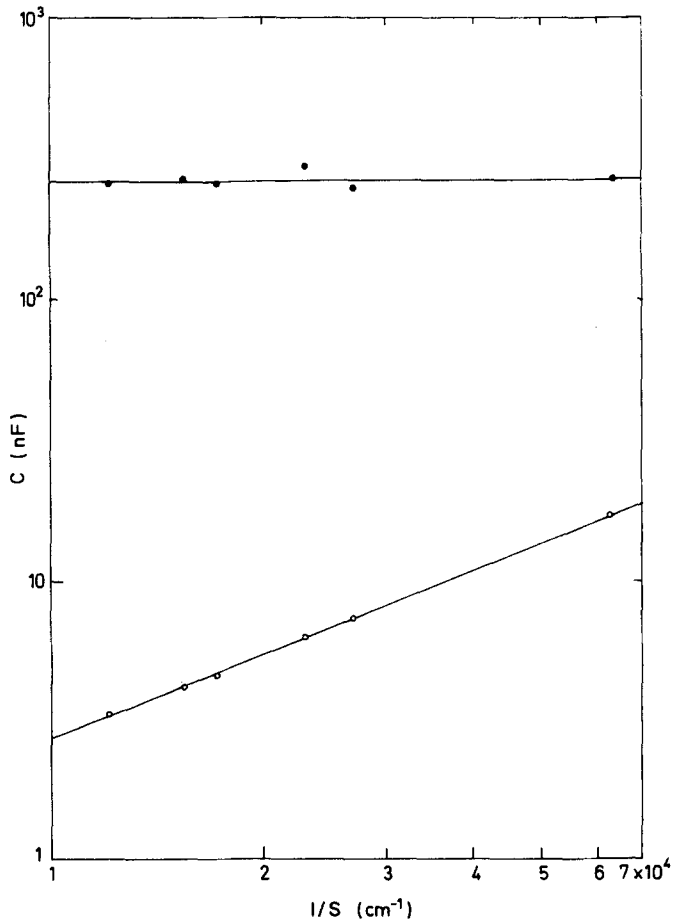

FIG. 2. Plot of capacitance-vs-inverse insulator thickness of Au-MoO_3-Au sample at 77 °K (lower curve) and 390 °K (upper curve).

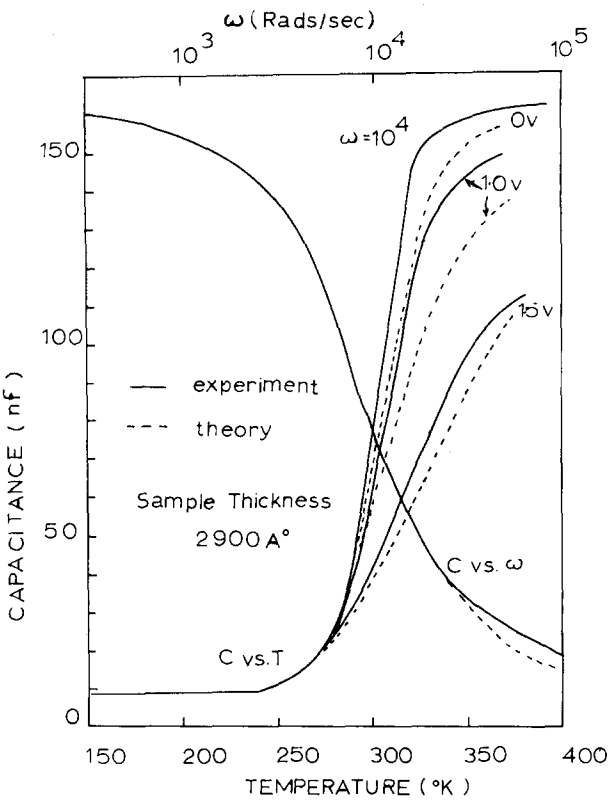

FIG. 3. C_p-vs-T ($\omega = 10^4$ rad/sec) and C_p-vs-ω ($T = 300$ °K, $V = 0$) for the Au-MoO_3-Au 2900-Å sample. The dotted lines represent the theoretical curve and the solid lines the experimental curves

(R_s) and the interior (R_b) may be assumed infinite. Thus, the data in this range represents the geometrical capacitance of the sample. On the other hand, at high temperature, R_b is very small and shunts the capacitance C_b of the interior of the insulator. Thus, the high-temperature capacitance is simply the series capacitance of the two Schottky barriers [see Eqs. (8) and (11)] which is, of course, independent of the thickness of the insulator. From the high-temperature capacitance the thickness of the barrier λ_{sc} is estimated to be about 160 Å. Using this value of λ_{sc} in Eq. (6) and using $\phi_0 = 1.5$ eV we obtain $N_0 \approx 10^{18}$ cm^{-3}.

The capacitance of the Au-MoO_3-Au samples as a function of temperature and frequency is shown in Fig. 3. These curves also provide information on the trap parameters and properties of the films. For example, using the value of $N_0 = 10^{18}$ cm^3, obtained above, ϕ_t was found to be equal to 0.28 eV to obtain the theoretical fits shown in Fig. 3. It is seen that the correlation between the theory and the experiment is extremely good, and leaves little doubt that the Schottky barrier model is valid in the case of the Au-MoO_3-Au system. (We note here that Al-CeF_3-Al and Al-Al_2O_3-Al samples show similar behavior.) The theoretical curves implicitly contain the effect of an electrode-limited to bulk-limited transition, occurring at 0.6 eV.[5,11]

B. Additional features of Schottky barrier model and a comparison with the data of Argall and Jonscher (Ref. 1)

A good deal of work has been carried out on the ac properties of silicon oxide films, the most comprehensive of which have been that of Argall and Jonscher.[1] These workers discussed their results in terms of the Debye model. Here, we reanalyze their data in terms of our model. The full curve in Fig. 4 shows tanδ-vs-frequency characteristics for Al-SiO-Al samples; the dotted curve illustrates the corresponding characteristics according to our model. There is no mistaking the similarities of the two sets of curves. Also, if the logarithm of the frequency corresponding to the dielectric loss peak is plotted against reciprocal temperature a straight line results. On the Debye model the behavior implies a rather artificial distribution of relaxation time with temperature:

$$\tau = \tau_0 \exp(-E/kT). \tag{21}$$

However, such a plot is a natural consequence of our model[4] since it may readily be shown that

$$\omega = [R_0^2 C_b (C_{sc} + C_b)]^{-1/2} \exp(-\phi_t/kT). \tag{22}$$

From Fig. 4 of Ref. 1, ϕ_t is found to be 0.64 eV. Also, using $C_s = 5.5 \times 10^{-8}$ pF and $C_b = 8 \times 10^{-10}$ pF [obtained from the low- and high-frequency C-vs-f plot of Fig. 3(b) of Ref. 1] and $R_0 = 10$ Ω (estimated from Fig. 4 of Ref. 1), we find the value for the intercept $[R_0^2 C_b (C_b + C_{sc})]^{-1/2}$ to be 1.3×10^7 sec^{-1}, which is in excellent agreement with the experimental value of 3×10^7 sec^{-1}.

Figures 5(a) and 5(b) illustrate the experimental curves, which represent the variation in tanδ and capacitance with voltage bias, with frequency as a parameter. The dotted lines in Figs. 5(a) and 5(b) are the theoretical curves obtained by using our model, and the values for C_{sc}, C_b, R_0, and ϕ_t were used for the theoretical curve in Fig. 4. It is quite evident that the theoretical and experimental curves are identical in nature. It is again noted here that the changes in capacitance, which is at least 60:1, *cannot* be accounted for on Debye model. Also, large changes in capacitance with voltage bias in itself is not supported on the basis of

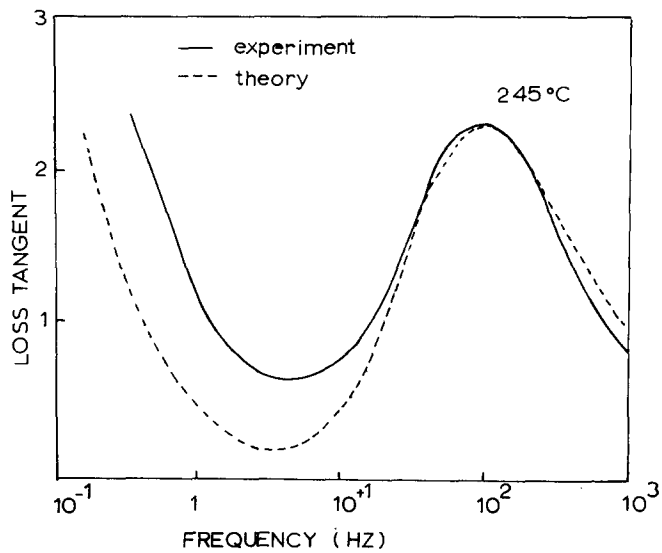

FIG. 4. Plots of tanδ-vs-frequency for Al-SiO-Al samples: Full curves are experimental curves (Ref. 1) and dotted curves are theoretical results.

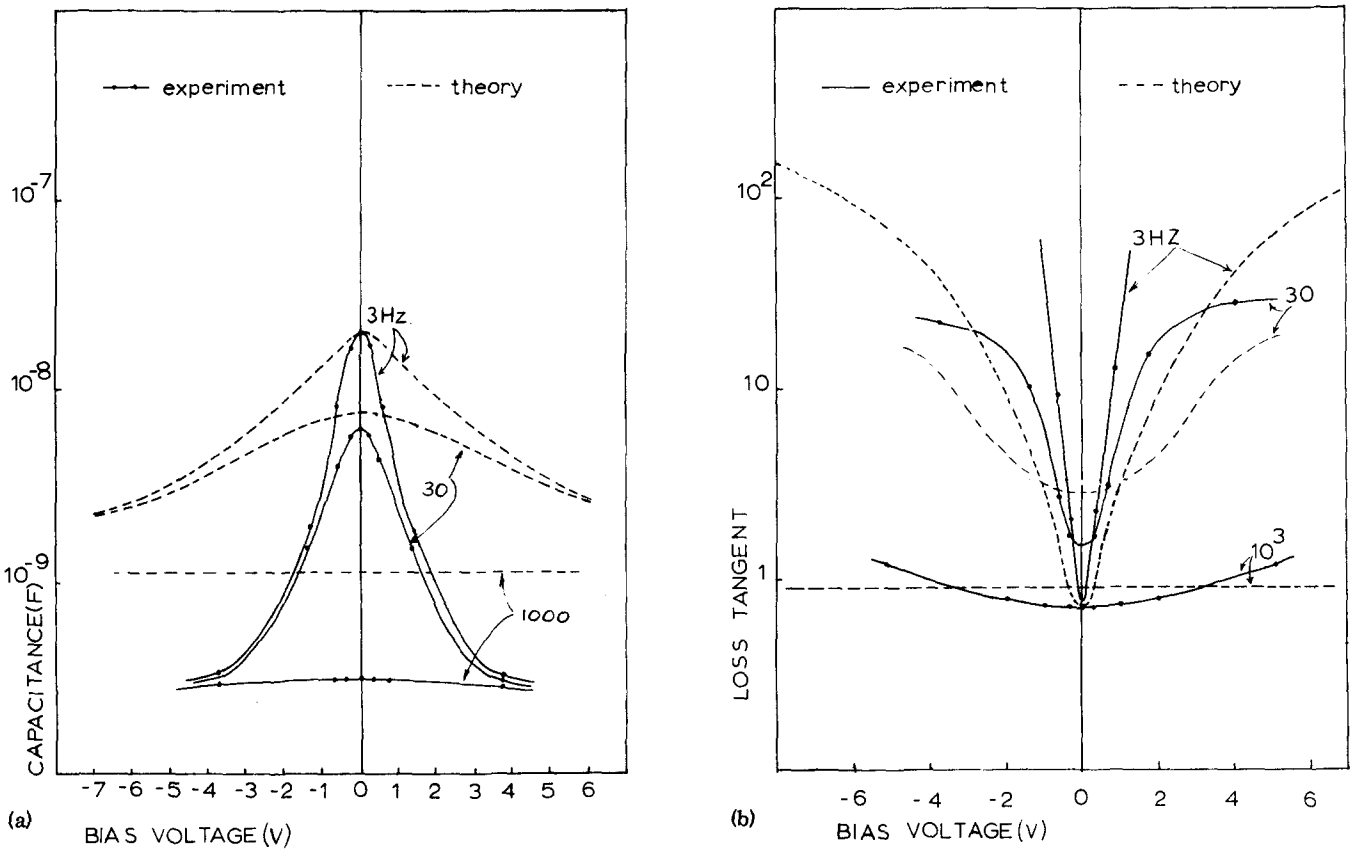

FIG. 5. Plots of (a) capacitance-vs-voltage bias and (b) tanδ-vs-voltage bias for Al-SiO-Al system. Solid lines are the experimental curves (Ref. 1) and dotted lines are the theoretical curves.

the Debye model. In constructing the theoretical curves it is again assumed that a contact-limited—to—bulk-limited transition occurs; Eqs. (1) and (2) were used for this purpose. [A value of $\phi_0 = 1.5$ eV was used in Eq. (2) and the transition voltage was 1.5 V.] This assumption is based on previous theoretical[8] and experimental work on SiO films[13,14] which supports the assumption. Without such a transition the theoretical curves are broader in nature than those shown.

When the underlying physical process is due to Debye-type relaxation, the experimental data conforms to a Cole-Cole plot; that is, if ϵ' is plotted as function of ϵ'' (for various frequencies) a *semicircle* results.[15] In point fact, the ϵ'-ϵ'' plot for the Al-SiO-Al samples does not conform even closely to a Cole-Cole plot, as shown in Fig. 6. This apparent anomaly, however, is a natural consequence of our model, incorporating the electrode-limited—to—bulk-limited transition that occurs in SiO films[8,13,14] as shown by the dotted curves in Fig. 6, which illustrates our theoretical ϵ'-ϵ'' curves [see Eqs. (17) and (19)] with voltage as a parameter. For $V = 0$, when the resistance of the contact is much higher than that of the bulk, the ϵ''-ϵ' characteristic is, in fact, a semicircle. Here we have used different values for C_s ($= 2.2 \times 10^{-9}$ pF) and $C_b + C_s$ ($= 2.3 \times 10^{-8}$ pF) in determining the low-frequency ϵ_1 ($= 12$) and the high-frequency ϵ_1 ($= 42$) in accordance with the experimental results in Fig. 19(a) of Argall and Jonscher's data.[15] However, as the voltage is increased and the contact resistance approaches that of the bulk, the characteristics deviates from being semicircular, the deviations occurring at decreasing values of ϵ' the greater the magnitude of V. The curves marked 1 V and 2 V represent the nature of the curves before and after the electrode-limited—to—bulk-limited transition has occurred ($V_T = 1.5$ V for this case). In the latter case the characteristic is never semicircular. Similar results would also pertain at zero bias, if the Schottky barriers were leaky.

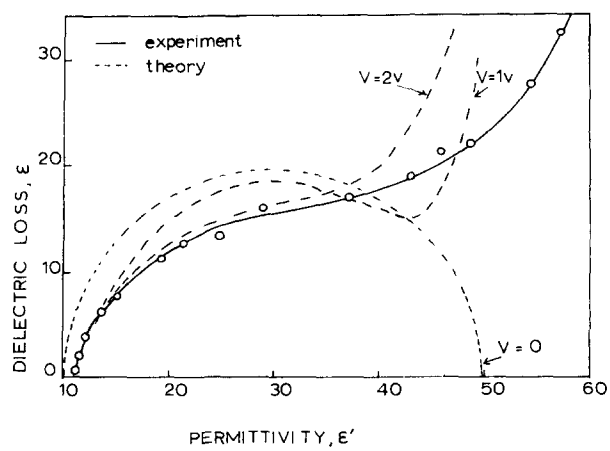

FIG. 6. Plot of ϵ'-vs-ϵ'' for various voltage biases for Al-SiO-Al samples. Solid lines are experimental curves (Ref. 1) and dotted lines are theoretical curves.

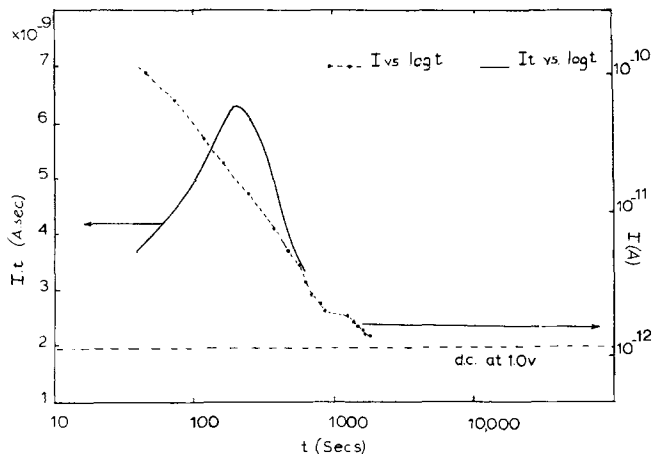

FIG. 7. I-vs-t and It-vs-t characteristics for Al-SiO-Al samples.

DISCUSSION

The theory of ac properties of the MIM system containing Schottky barriers at the metal-insulator interface has been presented. The theory has been shown to be compatible with experimental work carried out in the authors's laboratory.

The results of other workers have also been analyzed in light of our model and theory. These workers have attempted to explain the data on the basis of the Debye relaxation process on a *ad-hoc* basis, and no attempts were made to compare the theoretical and experimental characteristics. We have pointed out some gross inconsistencies in the data vis-a-vis the Debye theory. Furthermore, we have shown that all the data is consistent with our theory and, more to the point, that the data bears a striking resemblence to our theoretical curves, suggesting that our model may, in fact, be the operative one.

Additional support for our model comes from the I-t characteristics (decay curves where t is time) shown for SiO samples[1] for which ac data has been presented. We believe that the correlation of this characteristic with the ac characteristic is extremely important. We will now show that the information obtained from this curve is consistent with data obtained from the ac measurements assuming that our model is applicable in this case: It has been shown theoretically and experimentally[12] that when a step voltage is applied to a MIM system with Schottky barriers at the metal-insulator interfaces, initially the current through the system is a function of time before a steady-state current level is reached for the applied voltage. This is due to relaxation of the system from the nonsteady state to the steady state. The I-t characteristic of such a decay can provide information about the trap depth and trap distribution if the I-t curve is replotted as a product of the current and time-vs-log$t$ curve. In Fig. 7, we have replotted the experimental I-t characteristic (dotted curve) in the form of a It-t characteristic (solid curve). From the time t_m at which peak in It-t curve occurs we have calculated the trap depth ϕ_t to be 0.73 eV, using the expression[16]

$$\phi_t = kT \ln(\nu t_m), \tag{21}$$

where ν ($\approx 10^{10}$ sec^{-1}) is the attempt-to-escape frequency associated with the trap level.[17] This value is in good agreement with that calculated using ac data (0.7 eV), which provides further weight for the validity of our model.

*Study supported in part by National Research Council of Canada and Defence Research Board of Canada.
†Present address: Precision Electronic Components, Toronto 15, Canada.
[1]F. Argall and A.K. Jonscher, Thin Solid Films **2**, 185 (1968).
[2]Everszumrode and Rabus, Thin Solid Films **9**, 465 (1972).
[3]J.G. Simmons and G.S. Nadkarni, J. Vac. Sci. Technol **6**, 12 (1969).
[4]G.S. Nadkarni and J.G. Simmons, J. Appl. Phys. **41**, 545 (1970).
[5]G.S. Nadkarni and J.G. Simmons, J. Appl. Phys. **43**, 3741 (1972).
[6]F.S. Maddocks and R.E. Thun, J. Electrochem. Soc. **109**, 99 (1962).
[7]J.G. Simmons, J. Phys. Chem. Solids **32**, 1987 (1971); **32**, 2581 (1971).
[8]J.G. Simmons, Phys. Rev. **166**, 912 (1968).
[9]J.G. Simmons, G.S. Nadkarni, and M.C. Lancaster, J. Appl. Phys. **41**, 538 (1970).
[10]J.G. Simmons and G.S. Nadkarni, Phys. Rev. B **6**, 4815 (1972).
[11]G.S. Nadkarni and J.G. Simmons, J. Appl. Phys. **43**, 3650 (1972).
[12]G.S. Nadkarni and J.G. Simmons, Phys. Rev. B **7**, 3719 (1973).
[13]M. Stuart, Br. J. Appl. Phys. **18**, 1637 (1967).
[14]M. Stuart, Phys. Status Solidi **23**, 595 (1967).
[15]Figure 19 (a) of the data of Argall and Jonscher appears to be inconsistent with the other data that they present, in that the high-frequency ϵ_i is indicated to be 12, whereas elsewhere a value of 4.3 is suggested, and the low-frequency ϵ_1 is indicated to be 42, whereas a value of 100 would appear more appropriate. The latter anomaly is a consequence of extrapolating the apparent semicircular nature of the lower-frequency $\epsilon' - \epsilon''$ to higher frequencies. This procedure must lead to lower values for the high-frequency ϵ', as will be apparent from an inspection of our theoretical curves.
[16]J.C. Anderson, *Dielectrics* (Chapman and Hall, London, 1964).
[17]The value of ν was calculated using the relationship $\nu = v_{th}\sigma_n N_c$, where v_{th} ($\approx 10^7$ cm/sec for a trap with Coulombic barriers, as assumed here) is the thermal velocity, σ_n ($\simeq 10^{-16}$ cm^2) is the capture cross section of the trap. The value of 10^{-16} cm^2 is in good agreement with the experimental value obtained by Tam [M.A.Sc. (University of Toronto, 1971) (unpublished)].